Measuring the Total Radiated Energy of Transient Signals in a Reverberation Chamber

Qian Xu, Kai Chen, Xueqi Shen, Tian-Hong Loh, and Yi Huang

***Abstract*—For a continuous wave signal, the total radiated power (TRP) can be measured in a reverberation chamber (RC). In this paper, we show that the total radiated energy (TRE) can also be measured in an RC for transient signals, and the convergence speed is very fast for wideband signals. Measurements are performed to validate the proposed method.**

***Index Terms*—reverberation chamber, total radiated energy.**

I. Introduction

REVERBERATION chambers (RCs) have been widely used in electromagnetic compatibility (EMC) and over-the-air (OTA) testing in recent years [1]-[4]. Due to the inherent statistical properties, RCs are well suited for measuring global properties compared with anechoic chambers which are good at measuring angular-dependent properties. Typical measurements of RCs include: total radiated power (TRP) [5]-[7], total isotropic sensitivity (TIS) [2], [8], shielding effectiveness (SE) [9]-[12], antenna efficiency [13]-[17], diversity gain [18], [19], channel capacity [20], *etc*.

Most of the existing RC measurements work in a continuous wave mode, i.e. the time duration of the signal is much longer than the decay constant of an RC, and the fields in the RC can reach a steady state so that the instrument can perform measurements in the frequency domain (FD). However, for short-time pulses with non-sinusoidal signals, the power may vary so fast with time that the RC cannot reach a steady state. In this case, the power-time relationship of the radiated signal cannot be easily measured in an RC. In this paper, we show that an RC can still be used to measure the total radiated energy (TRE) of transient signals in the time domain (TD) without knowing the power-time relationship of the original signals. The working principle is similar to the total radiated power (TRP) measurement in RCs and the measurement setup is the same as TRP measurement except using different instruments. This method could be potentially useful to assess the TRE of high-power microwave devices.

The paper is organized as follows: the theory is presented in Section II, Section III provides measurement verifications. Discussion and conclusions are summarized in Section IV.

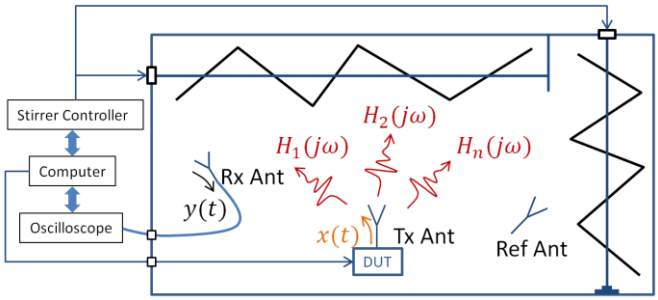

Fig. 1. A schematic plot of TRE measurement in an RC.

II. Theory

A schematic plot of the TRE measurement in an RC is illustrated in Fig. 1. As the transfer function (measured *S*-parameters) of an RC is defined in a 50 Ohm system, we assume

$$x(t)/\sqrt{50} = v_{\mathrm{rad}}(t)/\sqrt{R_{\mathrm{rad}}} \tag{1}$$

where $x(t)$ is the equivalent voltage in a 50 Ohm system of the radiated signal, $v_{\mathrm{rad}}(t)$ is the voltage signal on the radiation resistance R_{rad} of the transmitting (Tx) antenna. Thus, the TRE can be defined and expressed as

$$\mathrm{TRE} = \int_{-\infty}^{+\infty} \frac{x(t)^2}{50} dt \tag{2}$$

In the FD, for each stirrer position we have

$$Y_i(j\omega) = H_i(j\omega)X(j\omega) \tag{3}$$

where i represents different stirrer position (position index), $X(j\omega)$ is the frequency transform (FT) of $x(t)$, $Y_i(j\omega)$ is the FT of $y_i(t)$ (the received signal from the receiving (Rx) Ant in Fig. 1), and $H_i(j\omega)$ is the transfer function of the measurement system at each stirrer position. From (3) we have

This work was supported in part by the National Natural Science Foundation of China under Grants 61701224, and in part by Nanjing Rongce Testing Technology Ltd.

Q. Xu and K. Chen are with College of Electronic and Information Engineering, Nanjing University of Aeronautics and Astronautics, Nanjing 211106, China (e-mail: emxu@foxmail.com).

K. Chen and X. Shen are with Nanjing Rongce Testing Technology Ltd, Nanjing, 211112, China (e-mail: george@emcdir.com).

Y. Huang is with the Department of Electrical Engineering and Electronics, University of Liverpool, Liverpool L69 3GJ, U.K. (e-mail: yi.huang@liverpool.ac.uk)

T. –H. Loh is with Electromagnetic & Electrochemical Technologies Department, 5G & Future Communications Technology Group, National Physical Laboratory, Teddington, TW11 0LW, UK. (e-mail: tian.loh@npl.co.uk).

$$|Y_i(j\omega)|^2 = |H_i(j\omega)|^2 |X(j\omega)|^2 \quad (4)$$

By averaging (4) over different stirrer positions, we have $\langle|Y_i(j\omega)|^2\rangle = \langle|H_i(j\omega)|^2\rangle|X(j\omega)|^2$, thus

$$|X(j\omega)|^2 = \frac{\langle|Y_i(j\omega)|^2\rangle}{\langle|H_i(j\omega)|^2\rangle} \quad (5)$$

in a well-stirred RC, where $\langle\cdot\rangle$ represents the averaging operation over all stirrer positions ($i = 1, 2, \ldots, N$). From Parseval's theorem, (2) can be expressed as

$$\text{TRE} = \int_{-\infty}^{+\infty} \frac{x(t)^2}{50} dt = \int_{-\infty}^{+\infty} \frac{|X(j\omega)|^2}{50} df = \int_{-\infty}^{+\infty} \frac{\langle|Y_i(j\omega)|^2\rangle}{50\langle|H_i(j\omega)|^2\rangle} df \quad (6)$$

In practice, $|Y_i(j\omega)|$ can be measured using a real-time spectrum analyzer or $y_i(t)$ can be measured using a high sampling rate oscilloscope (in a 50 Ohm system). As long as $|Y_i(j\omega)|$ can be measured, $\langle|H_i(j\omega)|^2\rangle$ can be calibrated in the FD (same as that in the TRP measurement [2]), the TRE of the device under test (DUT) can be known quickly.

Suppose we use the same Rx Ant in the calibration process, $\langle|H_i(j\omega)|^2\rangle$ can be obtained in the FD using a reference antenna with known radiation efficiency

$$\langle|H_i(j\omega)|^2\rangle = \frac{\langle|S_{21}|^2\rangle}{\eta_{\text{Ref}tot}} \quad (7)$$

where $\eta_{\text{Ref}tot}$ is the total efficiency of the reference antenna (Ref Ant in Fig. 1), S_{21} represents the measured *S*-parameters at different stirrer positions between Ref Ant and Rx Ant.

III. Measurements

We demonstrate the validity of the proposed method using a vector network analyzer (VNA) due to the high dynamic range and high accuracy. Although the measurements were performed in the FD, the TD response can be obtained by using the inverse Fourier transform (IFT) to the FD results. The measurement setup is shown in Fig. 2. Ant 1 and Ant 2 were connected to Port 1 and Port 2 respectively, 100,001 frequency points were measured in the frequency range of 1 MHz - 10 GHz, two stirrers were rotated with 1°/step, *S*-parameters with 360 stirrer positions were recorded. The total efficiency of Ant 1 and Ant 2 has been measured using the three-antenna method [13] and is shown in Fig. 3(a).

To validate the proposed method, we can assume that the spectrum of the input signal is ideally bandlimited as shown in Fig. 3(b) and we use Ant 1 as the radiation source. The bandwidth of the spectrum is limited from 1 GHz to 2 GHz with an amplitude of 1. Considering the efficiency of Ant 1, the amplitude of the spectrum of the radiated signal becomes $\sqrt{\eta_{\text{Ant1}tot}}$, by applying IFT to $X(j\omega)$, the equivalent voltage

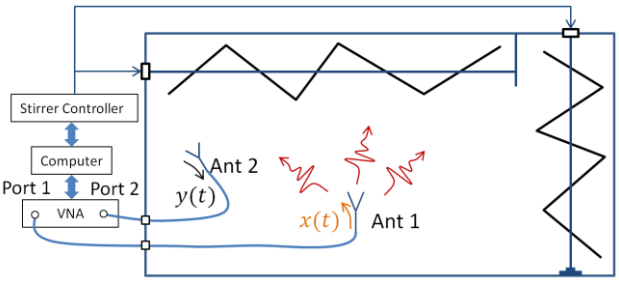

(a)

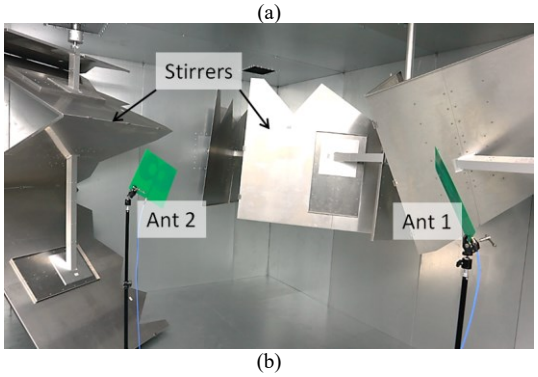

(b)

Fig. 2. Measurement setup: (a) schematic plot, (b) measurement in an RC, the inner dimensions of the RC are 6 m × 3.9 m × 2.8 m.

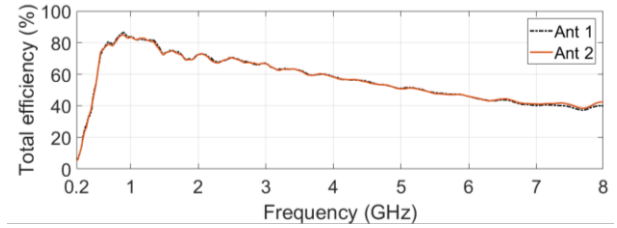

(a)

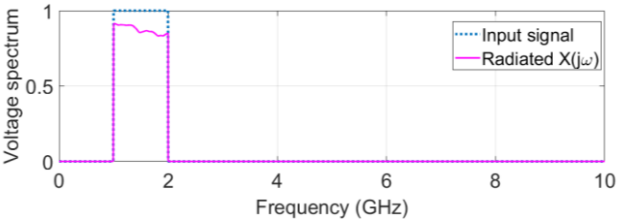

(b)

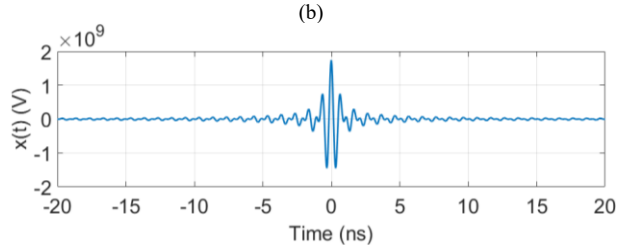

(c)

Fig. 3. Measurement results: (a) total efficiency of Ant 1 and Ant 2, (b) voltage spectrum of the input signal and the radiated signal, (c) the equivalent voltage of the radiated signal.

$x(t)$ of the radiated signal can be obtained in Fig. 3(c). The TRE can be directly calculated using (2), which is 3.05×10^7 J. In the next, we obtain the TRE from the received signals at the receiving antenna (Ant 2).

Because we use the same antenna (Ant 1) for transmitting and calibration, $\langle|H_i(j\omega)|^2\rangle$ in (6) (from the 'air port' to Port 2) can be obtained as

TABLE I
MEASUREMENT RESULTS

Bandwidth	Tx TRE	Measured TRE
1 GHz – 2 GHz	3.05×10^7 J	3.10×10^7 J
1 GHz – 8 GHz	1.57×10^8 J	1.59×10^8 J

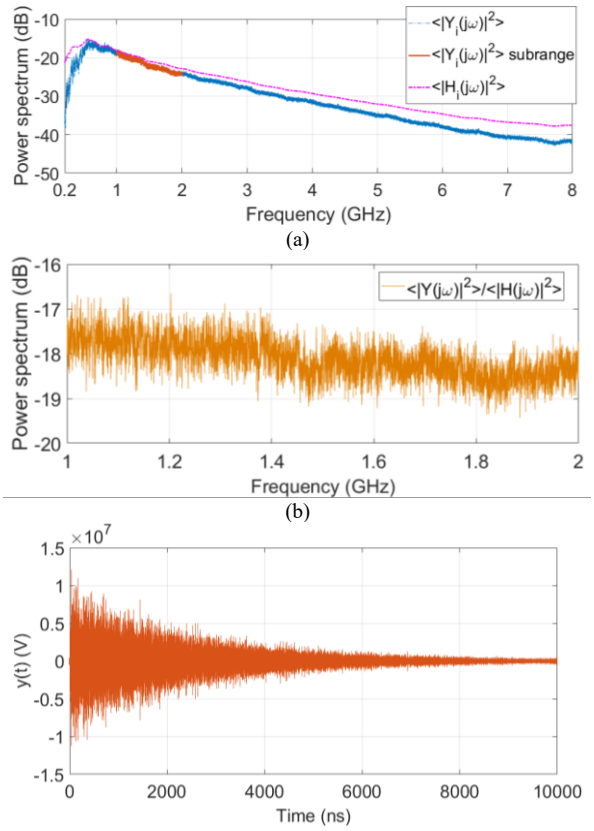

Fig. 4. Measurement results: (a) and (b) measured power spectrum, (c) measured TD signal.

$$\langle |H_i(j\omega)|^2 \rangle = T_{RC}\eta_{\text{Ant2}tot} = \frac{\lambda^3 Q}{16\pi^2 V}\eta_{\text{Ant2}tot} \qquad (8)$$

where T_{RC} is the chamber transfer function [3], $\eta_{\text{Ant2}tot}$ is the total efficiency of Ant 2, $Q = \omega\tau_{RC}$ is the quality factor of the RC, ω is the angular frequency, λ is the wavelength and V is the volume of the RC respectively. τ_{RC} was extracted using the TD technique [21], and the power spectrums of $\langle |H_i(j\omega)|^2 \rangle$ and the received signal $\langle |Y_i(j\omega)|^2 \rangle$ are illustrated in Fig. 4(a). Since the radiated TD signal is in the frequency range of 1 GHz - 2 GHz, the measured $\langle |Y_i(j\omega)|^2 \rangle / \langle |H_i(j\omega)|^2 \rangle$ can be calculated and is shown in Fig. 4(b). By applying the numerical integration in (6), the measured TRE can be obtained as 3.10×10^7 J, which agrees well with the value using the equivalent voltage from the Tx antenna (Ant 1). The small difference could be due to the uncertainty of antenna efficiencies.

The whole procedure was repeated for the TD signal covering the frequency bandwidth of 1 GHz - 8 GHz, and the results are summarized in Table I, which shows very good agreements. Convergence analysis for the stirrer position number is presented in Fig. 5, we use the results from 360 stirrer

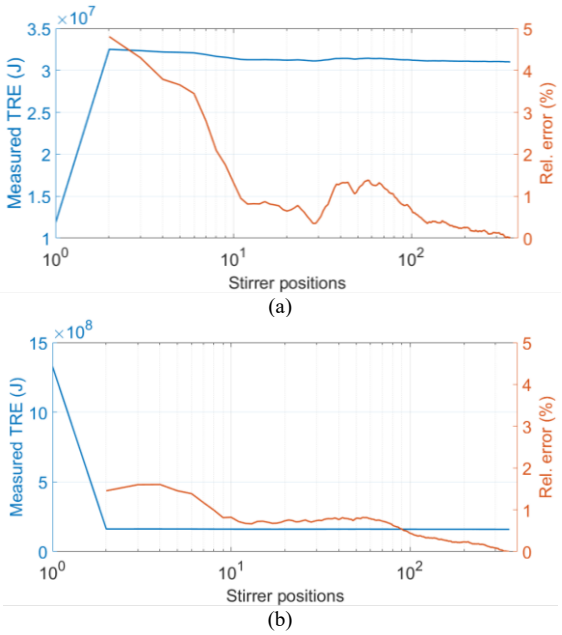

Fig. 5. Convergence analysis of the stirrer position number: (a) Tx signal with spectrum in 1 GHz - 2 GHz, (b) Tx signal with spectrum in 1 GHz - 8 GHz.

positions as references and calculate the relative errors. It is interesting to note that only two stirrer positions could be enough to have good accuracy (relative error < 5%). This is not surprising, if we check (6) carefully, we can find that the integral operator actually has the same effect with the frequency stirring technique (averaging over different frequencies). This also explains when the spectrum of the radiated signal becomes wider the relative error becomes smaller in Fig. 5(b). The wider the radiated spectrum is, the more independent sample number we have in the FD. Theoretically, according to the central limit theorem, the relative error is about $1/\sqrt{N \times M}$, where N is the independent stirrer position number and M is the independent frequency point number in the bandwidth. It is interesting to note that for a continuous wave signal, the bandwidth is zero, and (6) reduces to the equation in TRP measurement (by dividing the TRE by the duration of the signal). The error from only one stirrer position should be due to the unstirred part of the early time response which is not uniform for different positions in an RC.

Note that the radiated signals may be non-repetitive for different stirrer positions, in this case, more receiving antennas (source stirring) can be used simultaneously instead of mechanical stirring.

IV. CONCLUSIONS

We have demonstrated the validity of the measurement of TRE for transient signals in an RC. Theoretical equations and measurement results have been presented. The proposed method is very similar to the TRP measurement, and the equation reduces to the TRP measurement for continuous wave (or long time signals). We should also note that most of the radiated spectrum should fit the frequency range of the well-stirred condition of an RC, an insufficient number of independent samples or poor field uniformity may introduce

extra errors.

Because of the integral operator in the FD, it is interesting to note that the convergence speed of TRE measurement is very fast: only two stirrer positions could be enough for wideband signals.

REFERENCES

[1] IEC 61000-4-21, *Electromagnetic compatibility (EMC) – Part 4-21: Testing and measurement techniques – Reverberation chamber test methods,* IEC Standard, Ed 2.0, 2011-01.

[2] CTIA, *Test Plan for Wireless Large-Form-Factor Device Over-the-Air Performance*, ver. 1.2.1, Feb. 2019.

[3] D. A. Hill, *Electromagnetic Fields in Cavities: Deterministic and Statistical Theories*, Wiley-IEEE Press, USA, 2009.

[4] Q. Xu, Y. Huang, *Anechoic and Reverberation Chambers: Theory, Design, and Measurements*, Wiley-IEEE Press, USA, 2019.

[5] T. Jia, Y. Huang, Q. Xu, Q. Hua, and L. Chen, "Average Rician K-factor based analytical uncertainty model for total radiated power measurement in a reverberation chamber," *IEEE Access*, vol. 8, pp. 198078-198090, 2020.

[6] Q. Xu, W. Qi, C. Liu, L. Xing, D. Yan, Y. Zhao, T. Jia, and Y. Huang, "Measuring the total radiated power of wideband signals in a reverberation chamber," *IEEE Antennas and Wireless Propagation Letters*, vol. 19, no. 12, pp. 2260-2264, Dec. 2020

[7] W. Xue, F. Li, X. Chen, S. Zhu, A. Zhang, and T. Svensson, "A unified approach for uncertainty analyses for total radiated power and total isotropic sensitivity measurements in reverberation chamber," *IEEE Transactions on Instrumentation and Measurement*, vol. 70, pp. 1-12, 2021.

[8] X. Chen, W. Xue, H. Shi, J. Yi, and W. E. I. Sha, "Orbital angular momentum multiplexing in highly reverberant environments," *IEEE Microwave and Wireless Components Letters*, vol. 30, no. 1, pp. 112-115, Jan. 2020.

[9] C. L. Holloway, D. A. Hill, M. Sandroni, J. M. Ladbury, J. Coder, G. Koepke, A. C. Marvin and Y. He, "Use of reverberation chambers to determine the shielding effectiveness of physically small, electrically large enclosures and cavities," *IEEE Transactions on Electromagnetic Compatibility*, vol. 50, no. 4, pp. 770-782, Nov. 2008.

[10] C. L. Holloway, D. A. Hill, J. Ladbury, G. Koepke and R. Garzia, "Shielding effectiveness measurements of materials using nested reverberation chambers," *IEEE Transactions on Electromagnetic Compatibility*, vol. 45, no. 2, pp. 350-356, May 2003.

[11] A. Gifuni and M. Migliaccio, "Use of nested reverberating chambers to measure shielding effectiveness of nonreciprocal samples taking into account multiple interactions," *IEEE Transactions on Electromagnetic Compatibility*, vol. 50, no. 4, pp. 783-786, Nov. 2008.

[12] Z. Tian, Y. Huang and Q. Xu, "Efficient methods of measuring shielding effectiveness of electrically large enclosures using nested reverberation chambers with only two antennas," *IEEE Transactions on Electromagnetic Compatibility*, vol. 59, no. 6, pp. 1872-1879, Dec. 2017.

[13] C. L. Holloway, H. A. Shah, R. W. Pirkl, F. Young, D. A. Hill and J. Ladbury, "A three-antenna technique for determining the total and radiation efficiencies of antennas in reverberation chambers", *IEEE Antennas Propag. Mag.*, vol. 54, no. 1, pp. 235-241, Jun. 2012.

[14] W. Xue, X. Chen, M. Zhang, L. Zhao, A. Zhang and Y. Huang, "Statistical analysis of antenna efficiency measurements with non-reference antenna methods in a reverberation chamber," *IEEE Access*, vol. 8, pp. 113967-113980, 2020.

[15] D. Yan, Q. Xu, C. Yu, Y. Huang, and T. H. Loh, "A broadband reference antenna for efficiency measurements in a reverberation chamber," *IEEE 3rd International Conference on Electronic Information and Communication Technology (ICEICT)*, Shenzhen, China, 2020, pp. 302-305.

[16] Q. Xu, L. Xing, Z. Tian, Y. Zhao, X. Chen, L. Shi and Y. Huang, "Statistical distribution of the enhanced backscatter coefficient in reverberation chamber," *IEEE Transactions on Antennas and Propagation*, vol. 66, no. 4, pp. 2161-2164, April 2018.

[17] C. Li, T. -H. Loh, Z. Tian, Q. Xu and Y. Huang, "Evaluation of chamber effects on antenna efficiency measurements using non-reference antenna methods in two reverberation chambers," *IET Microwaves, Antennas & Propagation*, vol. 11, no. 11, pp. 1536-1541, 2017.

[18] J. Yang, S. Pivnenko, T. Laitinen, J. Carlsson and X. Chen, "Measurements of diversity gain and radiation efficiency of the Eleven antenna by using different measurement techniques," *Proceedings of the Fourth European Conference on Antennas and Propagation*, Barcelona, Spain, 2010, pp. 1-5.

[19] Q. Xu, Y. Huang, X. Zhu, S. S. Alja'afreh and L. Xing, "A new antenna diversity gain measurement method using a reverberation chamber," *IEEE Antennas and Wireless Propagation Letters*, vol. 14, pp. 935-938, 2015.

[20] X. Chen, P. Kildal, J. Carlsson and J. Yang, "Comparison of ergodic capacities from wideband MIMO antenna measurements in reverberation chamber and anechoic chamber," *IEEE Antennas and Wireless Propagation Letters*, vol. 10, pp. 446-449, 2011.

[21] Q. Xu, Y. Huang, Y. Zhao, L. Xing, Z. Tian, and T. H. Loh, "Investigation of bandpass filters in the time domain signal analysis of reverberation chamber," *XXXIInd General Assembly and Scientific Symposium of the International Union of Radio Science (URSI GASS)*, Montreal, QC, Canada, 2017, pp. 1-4.